Structural and electronic properties of the one-dimensional organic metal bis(thiodimethylene)-tetrathiafulvalene tetracyanoquinodimethane

C. Rovira, J. Tarrés, J. Llorca, E. Molins, and J. Veciana
Institut de Ciència de Materials de Barcelona (CSIC), Campus de la Universitat Autonoma de Barcelona, 08193 Bellaterra, Spain

S. Yang and D. O. Cowan
Department of Chemistry, The Johns Hopkins University, Baltimore, Maryland 21218

C. Garrigou-Lagrange, J. Amiell, and P. Delhaes
Centre de Recherche Paul Pascal, Chateau Brivazac, 33600 Pessac, France

E. Canadell
Laboratoire de Chimie Théorique (CNRS URA 506), Université de Paris-Sud, 91405 Orsay, France

J. P. Pouget
Laboratoire de Physique des Solides (CNRS UA 040002), Université de Paris-Sud, 91405 Orsay, France
(Received 5 April 1995)

The synthesis and structural characterization at room temperature and 130 K of the organic charge-transfer salt bis(thiodimethylene)-tetrathiafulvalene tetracyanoquinodimethane (BTDMTTF-TNCQ) is reported. X-ray diffuse scattering as well as ir and Raman measurements show that the charge transfer in this salt is ~ 0.5. BTDMTTF-TCNQ remains metallic down to very low temperatures but exhibits an anomaly at 175 K in the conductivity and thermopower which could be related to some unusual structural modification of the unit cell. Band-structure calculations show that this salt is a narrow-band one-dimensional metal. The high value of the spin susceptibility, the low value of the conductivity, and the observation of a $4k_F$ charge-density-wave (CDW) instability around room temperature prove that it is a highly correlated metal. In contrast with other salts of the TTF-TCNQ family, BTDMTTF-TCNQ does not exhibit critical $2k_F$ structural fluctuations. It is proposed that the absence of the $2k_F$ CDW transition is due to the stronger interlocking of the donor and acceptor molecules due to the presence of the sulfur atoms in the central position of the outer five-membered rings of the BTDMTTF donor.

I. INTRODUCTION

The synthesis of TTF-TCNQ (tetrathiafulvalene-tetracyanoquinodimethane)[1] in 1973 opened a vast area of research which more than 20 years later remains still lively and exciting. The charge-transfer salt TTF-TCNQ was not only the first truly organic metal, but also a prototypical material where the physics of one-dimensional (1D) metals, by then almost unexplored, could be studied. A wealth of chemical and physical techniques was used to characterize this salt.[2,3] TTF-TCNQ is a molecular metal with a partial charge transfer of $\rho = 0.55-0.59$ electrons from the donor (TTF) to the acceptor (TCNQ). It exhibits several phase transitions at 54, 49, and 38 K which successively destroy the metallic conductivity on the TCNQ and TTF chains. X-ray diffuse scattering measurements showed that TTF-TCNQ exhibits both $2k_F$ and $4k_F$ charge-density-wave (CDW) structural fluctuations, the latter being associated with TTF chains[4] (k_F is the Fermi wave vector of the 1D electron gas). Thus one of the more interesting aspects of this salt was the possibility to study the electronic instabilities of two correlated 1D electron gases located on the donor and acceptor stacks and their interaction (via electron-phonon coupling) with the lattice degrees of freedom.

The rich physics exhibited by TTF-TCNQ stimulated a continuous interest in preparing other molecular charge-transfer salts of the same type by carrying out slight chemical modifications of the two molecular partners. Thus, TSF-TCNQ (tetraselenafulvalene-tetracyanoquinodimethane), HMTTF-TCNQ (hexamethylenetetrathiafulvalene-tetracyanoquinodimethane), TMTTF-TCNQ (tetramethyltetrathiafulvalene-tetracyanoquinodimethane), and TMTSF-DMTCNQ (tetramethyletraselenafulvalene-dimethyletracyanoquinodimethane), to name a few, were synthesized and their physical properties were studied in detail.[2,3] All these 1D salts were found at low temperature to undergo a $2k_F$ CDW Peierls transition toward an insulating ground state. In one of them however, TMTSF-DMTCNQ, it was found that pressure can remove the metal-insulator phase transition and thus stabilize a metallic state until very low temperatures.[5] A similar feature was found to occur in the 2:1 cation radical salts of the TMTSF family, and with the stabilization of a metallic state in pressurized $(TMTSF)_2PF_6$ the organic superconductivity was discovered.[6] This discovery has raised a considerable number of studies of 2:1 cation radical salts based on the TMTSF donor and its chemical modifications,[7] where a

charge transfer of one electron from two donor molecules to an inorganic anion is achieved.

In recent years 1D salts, in which there is a partial charge transfer from the donor stacks to the acceptor stacks, were synthesized and shown to display a remarkable variety of physical behaviors. For example, superconductivity was observed in pressurized TTF-$[M(dmit)]_2$ with M =Ni and Pd,[8] and, at ambient pressure, metallic behavior was also found down to a few degrees K in TTeF-TCNQ (tetratellurafulvalene-tetracyanoquinodimethane)[9] and TSeT-BTDATCNQ [tetraselenotetracene-bis(1,2,5-thiadiazolo)tetracyanoquinodimethane].[10] Some aspects of the physics of these 1D metals are still not yet fully understood. Thus there is a need to prepare and characterize materials of this type. Recently we have synthesized the BTDMTTF [bis(thiodimethylene)-tetrathiafulvalene] donor[11] as well as its TCNQ charge-transfer salt.[12] The BTDMTTF molecule can be described as a HMTTF (hexamethylenetetrathiafulvalene) donor where the central CH_2 group of the five-membered ring has been replaced by an S atom. Preliminary studies[12] indicate that the TCNQ salt is 1D and also remains metallic down to low temperatures.

In this paper we report the preparation and the crystal and electronic structures of BTDMTTF-TCNQ, together with a study of its transport, magnetic, and optical properties and a search for eventual structural instabilities.

II. SAMPLE PREPARATION

BTDMTTF was synthesized as previously reported,[11] and TCNQ was purchased from Aldrich Co. and recrystallized before use. High-purity solvents ($>99.9\%$) were dried and then fractionally distilled under nitrogen. Shiny black needles $[(5.5-0.3)\times(0.6-0.4)\times(0.08-0.02)$ mm^3) of BTDMTTF-TCNQ have been prepared by carefully layering a carbon disulfide/BTDMTTF solution with an acetonitrile/TCNQ solution (2×10^{-3} M each) in a straight cell.

III. CRYSTAL STRUCTURE

A high-quality crystal of $0.36\times0.38\times0.06$ mm^3 was selected for the x-ray-diffraction experiments. X-ray data were collected on an Enraf-Nonius CAD-4 diffractometer with graphite monochromatized Mo $K\alpha$ radiation. At room temperature (RT) 2523 reflections were measured up to $2\theta=60°$ using an ω-2θ scan mode, among which 1600 were unique $[-30\le h\le 30, 0\le k\le 17, 0\le 1\le 5]$. With the criterion $I>2.5\sigma(I)$, 1174 reflections were considered to be observed and used for the refinement process. The standard reflection decay during the experiment was 0.58%. The structure was solved by direct methods[13] and refined by the full-matrix least-square methods.[14] Hydrogen atoms were located by difference Fourier synthesis and, at the final stage, all atoms were refined with anisotropic thermal parameters. Refinement with 106 parameters converged at $R=0.033$ and $wR=0.037[w=1/\sigma^2(F)+0.001\,647F^2)]$. The maximum and minimum peak heights in the last difference Fourier synthesis were 0.50 and -0.43 e Å^{-3}.

Low-temperature high-resolution x-ray-diffraction experiments were done using a nitrogen low-temperature device. 21505 reflections were measured at 130(3) K up to $(\sin(\theta)/\lambda)_{max}$ of 1.35 Å^{-1}. After the averaging 6885 reflections were obtained,[15] $R_{int}(F^2)=0.017$ and 5145 with $F>3\sigma(F)$. A refinement[16] on F^2 converged to $wR2=0.082[R1=0.033$ for $5646F_0>4\sigma(F_0)]$. The final difference Fourier synthesis shows electron-density peaks located in bonding regions. An electron-density distribution study of this complex is now in progress and will be published elsewhere.

BTDMTTF-TCNQ crystallizes in the monoclinic system $C2/m$ and is isostructural with HMTSF-TCNQ.[17] Its structure is also closely related to the orthorhombic $Pmma$ one of HMTTF-TCNQ.[18] Table I compares the lattice parameters of these three charge-transfer salts. The atomic coordinates (for labeling, see Fig. 1) and equivalent isotropic displacement parameters for BTDMTTF-TCNQ at RT and 130 K are listed in Table II.

The crystal structure is dominated by uniform, segregated stacks of donors and acceptors which propagate along the crystallographic c axis. As it is particularly visible in the (001) crystallographic projection [Fig. 2(a)], the mode of interchain packing in BTDMTTF-TCNQ is such that each donor column is surrounded by four acceptor columns, and vice versa. Within each stack, adjacent molecules exhibit the commonly observed ring-over-bond overlap arrangement[19] (Fig. 3). At RT, the mean interplanar separations in the donor (3.58 Å) and

TABLE I. Crystallographic data of BTDMTTF-TCNQ at RT and 130 K compared to those of HMTSF-TCNQ (Ref. 17) and HMTTF-TCNQ (Ref. 18) at RT.

	BTDMTTF-TCNQ		HMTSF-TCNQ	HMTTF-TCNQ
	298 K	130 K	RT	RT
Space group	$C2/m$	$C2/m$	$C2/m$	$Pmma$
a(Å)	21.296(7)	21.205(2)	21.999(14)	12.462(4)
b(Å)	12.567(8)	12.530(2)	12.573(8)	3.901(2)
c(Å)	3.928(1)	3.859(1)	3.980(1)	21.597(6)
β(o)	92.74(2)	93.30(1)	90.29(4)	90.00
V(Å^3)	1050	1023.6	1076	1050
Z	2		2	2
D_{calc}(g cm^{-3})	1.663	1.70	2.087	1.546
MW	524.7		676.3	488.7

TABLE II. Atomic coordinates ($\times 10^4$) and equivalent isotropic displacement parameters ($Å^2 \times 10^3$) for BTDMTTF-TCNQ at 298 and 130 K. U_{eq} is defined as one-third of the trace of the orthogonalized U_{ij} tensor.

	130 K				298 K			
Atom	x	y	z	U_{eq}	x	y	z	U_{eq}
S(2)	9309(1)	−1181(1)	1554(1)	11(1)	9211(1)	−1176(1)	1552(1)	30(1)
S(5)	7589(1)	0	5769(1)	11(1)	7599(1)	0	5758(2)	30(1)
N(10)	6598(1)	−1793(1)	−500(2)	19(1)	6595(1)	−1764(2)	−441(6)	45(1)
C(1)	9707(1)	0	674(2)	10(1)	9706(1)	0	671(8)	27(1)
C(3)	8644(1)	−538(1)	2970(1)	10(1)	8652(1)	−534(2)	2989(5)	26(1)
C(4)	8065(1)	−1084(1)	4132(1)	11(1)	8074(1)	−1079(2)	4154(6)	29(1)
C(6)	5286(1)	−982(1)	4110(1)	11(1)	5267(1)	−976(2)	4109(6)	29(1)
C(7)	5560(1)	0	3144(2)	10(1)	5557(1)	0	3162(7)	26(1)
C(8)	6105(1)	0	1267(2)	10(1)	6104(1)	0	1306(7)	27(1)
C(9)	6391(1)	−972(1)	294(1)	12(1)	6390(1)	−972(2)	343(6)	31(1)
H(41)	7846(5)	−1445(10)	2097(31)	17(2)	7870(11)	−1432(21)	2192(80)	43(1)
H(42)	8160(5)	−1596(9)	6126(26)	14(2)	8169(11)	−1543(23)	6089(66)	37(1)
H(6)	5462(6)	−1634(10)	3536(29)	19(3)	5461(11)	−1621(21)	3480(56)	32(1)

acceptor (3.26 Å) stacks are identical to those of HMTTF-TCNQ.[18] These distances are shorter at 130 K: 3.451 and 3.186 Å for the donor and acceptor stacks, respectively. The molecule of TCNQ is planar, whereas BTDMTTF has external sulfur atoms (S5) tilted up and down from the molecular mean plane by 9.62°.

Upon examination of Fig. 2(b), it is also clear that the tilts of the donor (24.27° at RT) and acceptor (33.86° at RT) molecules with respect to the stack axis c are not so different, leading to an interplanar dihedral angle of 9.58°. One of the consequences of the near coplanarity of donors and acceptors in the crystal packing arrangement is the existence of short interchain contacts along b [see Fig. 2(a)] involving the internal sulfur atoms (S2) of the donor and the nitrogen of the acceptor (3.24 Å). As in other salts of this series,[9] there are also C-H (donor) · · · N contacts which are either shorter (2.643 Å) or of the same order (2.760 Å) as the sum of the van der Waals radii. The S · · · N contacts are similar to those found in HMTTF-TCNQ (3.25 Å),[18] but larger than those existing in the isostructural HMTSF-TCNQ (Se · · · N, 3.10 Å).[17] On the other hand, the external sulfur atom (S5) of BTDMTTF does not have short contacts with the nitrogen atom in the nearest TCNQ

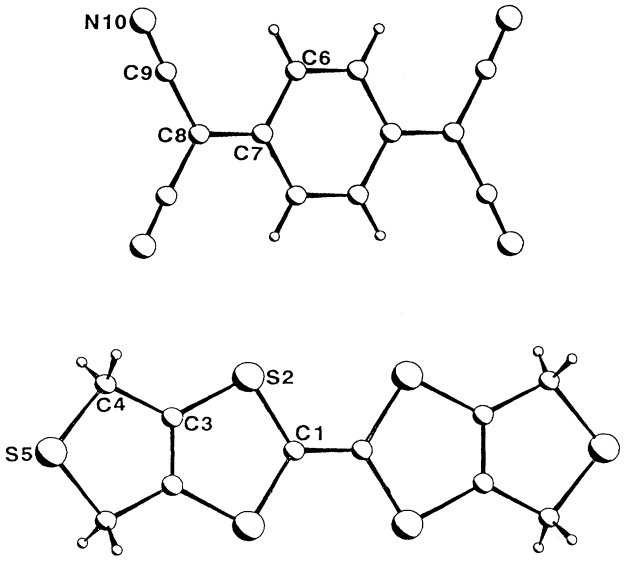

FIG. 1. Molecular structures of TCNQ and BTDMTTF showing the atom labeling.

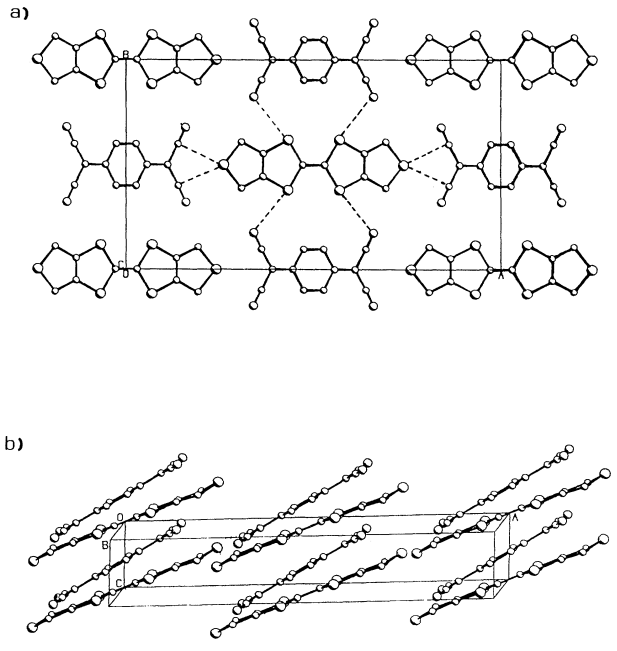

FIG. 2. Crystal structure of BTDMTTF-TCNQ: (a) projection along the c axis showing short S · · · N and S · · · C intermolecular contacts; (b) projection along the b axis.

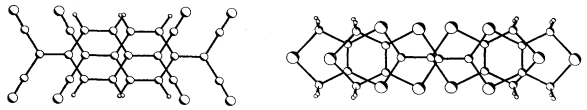

FIG. 3. Intrastack molecular overlap pattern of the TCNQ (left) and BTDMTTF (right) molecules.

(S · · · N, 3.467 Å), but the distance from the carbon atom (C9) of the C≡N group along *a* (S · · · C, 3.44 Å) is shorter than the sum of the van der Waals radii. All these short contacts make the structure of BTDMTTF-TCNQ very compact. This can be also seen in Table I: the unit-cell volume of BTDMTTF-TCNQ at RT is identical to that of HMTTF-TCNQ in spite of the presence of a bulkier donor (for further discussion of this point, see Sec. IX).

The thermal dependence of the unit-cell parameters has been measured between RT and 130 K. A very unusual behavior consisting in a larger rate of decrease of *a*, *b*, and *c* and a larger rate of increase of β is observed below about 175 K. Among them, the stacking axis *c* suffers the largest relative variation (Fig. 4). It is also noteworthy that the tilt angle decreases similarly in the donor (from 24.27° at RT to 22.67° at 130 K) and acceptor (from 33.86° at RT to 31.11° at 130 K) stacks. As a consequence the interplanar dihedral angle varies only very slightly (from 9.58° at RT to 9.33° at 130 K) with temperature. This maintains the compact packing of molecules.

IV. TRANSPORT PROPERTIES

A. Conductivity

Measurements were performed on samples with dimensions of (1.5–2.00)×(0.4–0.6)×(0.03–0.04) mm^3. Crystals were mounted with four probes on PC boards with

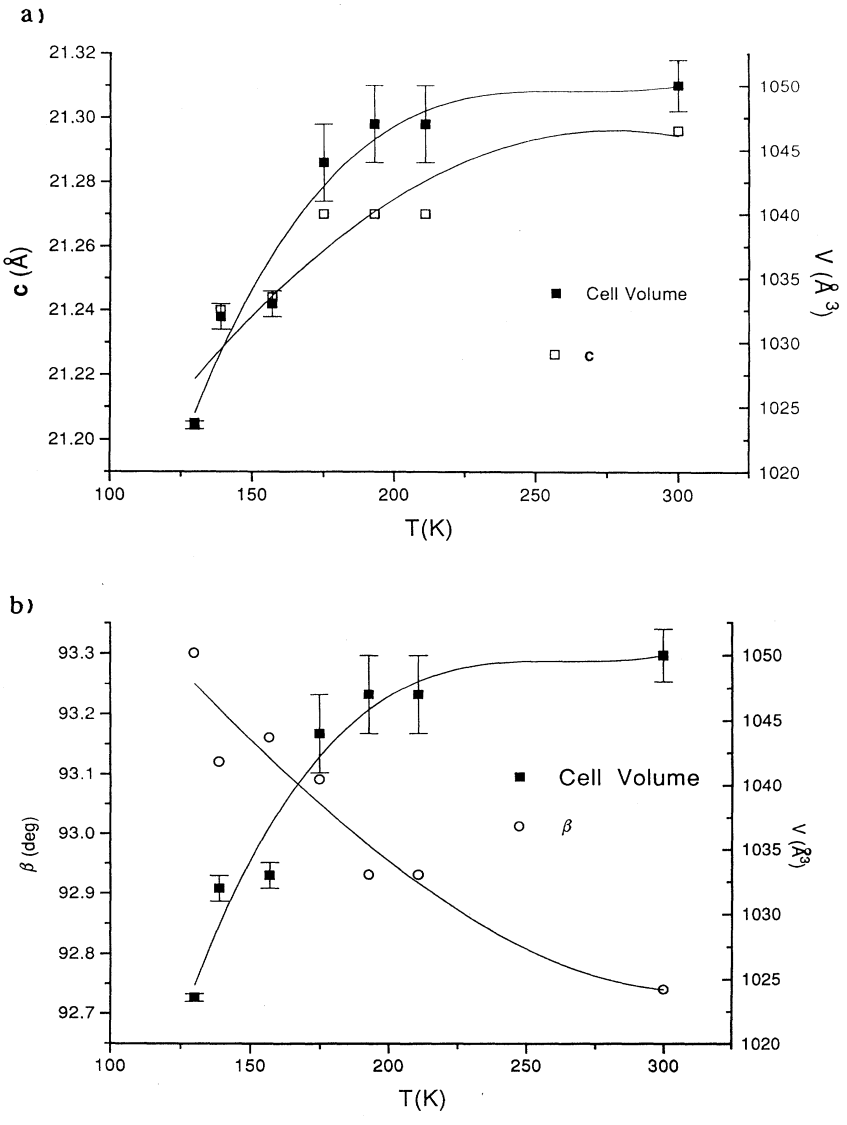

FIG. 4. Thermal dependence of the lattice parameters of BTDMTTF-TCNQ: (a) Cell volume (with e.s.d.s) and *c* axis. (b) Cell volume and β angle. Lines correspond to polynomial fits (only to guide the eye).

12.7-μm gold wires. In order to avoid wire stress to the contacts, small kinks in the wires were made. DuPont 4929 silver paste was mixed with 2-butoxyethyl acetate as a thinner for mounting contacts. The PC board was then attached onto a sample holder which was placed inside of a quasi-isothermal copper can in a constant flow cryostat. A LakeShore Cryotonics DRC82C temperature controller was connected to the sample holder and the copper can to maintain a constant rate of 0.5° per minute temperature change. A Keithley 220 programmable current source was installed for supplying current to the samples. The current was reversed and the voltage readings were averaged to remove any extraneous values. Voltage measurements were made with a Keithley 181 nanovoltmeter for metallic samples, and a Keithley 619 electrometer for semiconducting samples. The data were collected every 0.05° from room temperature down to liquid-helium temperatures. The temperature change, current supply, voltage measurement, and data collection were automatically controlled and managed by a HP9816A computer/HP9121D disc drive.

The RT conductivity of BTDMTTF-TCNQ is of 130 S/cm, about four times smaller than that of TTF-TCNQ or HMTTF-TCNQ ($\sim$500 S/cm), and more than one order of magnitude smaller than that of HMTSF-TCNQ (1800 S/cm).[2,3] The dc measurements of Fig. 5 show that the resistivity of BTDMTTF-TCNQ decreases upon cooling. After a rapid decrease below RT, its rate of decrease saturates below about 175 K, and a broad minimum of resistivity occurs around 25 K. At this temperature the conductivity 1100 S/cm is 8.5 times the RT value. Below 25 K the resistivity increases slightly. No evidence of a metal-insulator Peierls transition is shown by the conductivity measurements down to 4 K.

B. Thermoelectric power

The measurements were performed on crystals with dimensions of $(1.3-1.6)\times(0.03-0.06)\times(0.03-0.05)$ mm^3 that were mounted with 25.4-μm pure gold wires (99.99%, California Fine Wire Co.) and DuPont 4929 silver paste onto a thermoelectric power device. A Keithley 220 current source supplied with $\sim$1-mA current to the heater of the device which made the temperature difference between both ends of the sample $\sim$1 K. The thermocouple was made with gold and chromel wires. Readings of the voltage from the thermocouple were monitored by a Hewlett Packard 3497 A microvoltmeter. A Keithley 181 nanovoltmeter was operated to measure the thermoelectric voltage of the sample. The temperature controlling throughout the experiment was performed with a LakeShore Cryotonics DRC 82C temperature controller. The data collection for the experiment was done by a HP9816A computer/HP9121D disc drive from room temperature down to liquid-helium temperature.

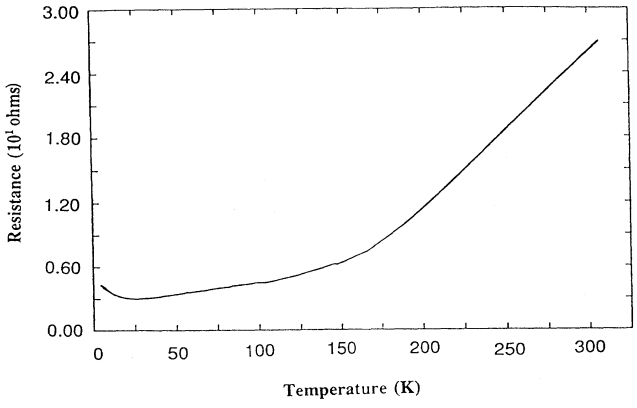

FIG. 5. Thermal dependence of the longitudinal resistance of BTDMTTF-TCNQ.

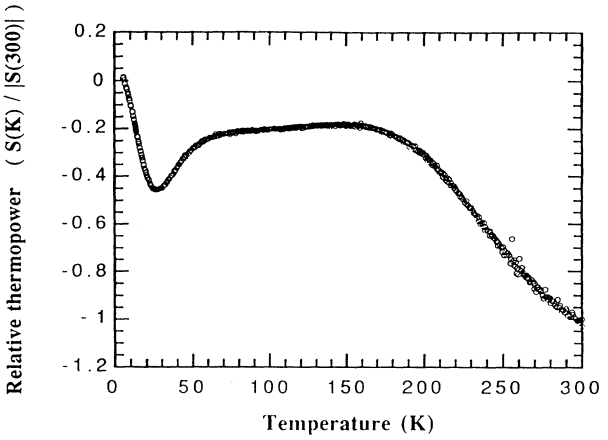

FIG. 6. Thermal dependence of the relative thermopower $S(T)/|S(300\text{ K})|$ of BTDMTTF-TCNQ.

The thermopower $S(T)$ of BTDMTTF-TCNQ is negative, which indicates that the main charge carriers are the electrons on the TCNQ stacks. Its thermal variations normalized to its RT absolute value are shown in Fig. 6. The thermal behavior of the thermopower recalls that of the electrical conductivity. The increase of $S(T)$ stops at about the same temperature (175 K) at which the conductivity flattens. $S(T)$ slightly decreases below this temperature, and at about 25 K shows an upturn in its thermal dependence. Such an upturn is also exhibited by the electrical conductivity in the same temperature range.

V. MAGNETIC PROPERTIES

The static susceptibility has been measured between 300 and 4 K using a standard Faraday balance. After correction for the core diamagnetic component calculated from usual Pascal constants, a RT contribution of the conduction electrons to the susceptibility of 7.1×10^{-4}-emu cgs mol (χ_p) was determined. This value is slightly larger than that of TTF-TCNQ (6×10^{-4} emu cgs mol), and about three times larger than that of HMTTF-TCNQ (2.4×10^{-4} emu cgs mol).[2,20] Figure 7 shows that χ_p decreases dramatically upon cooling. A similar rate of de-

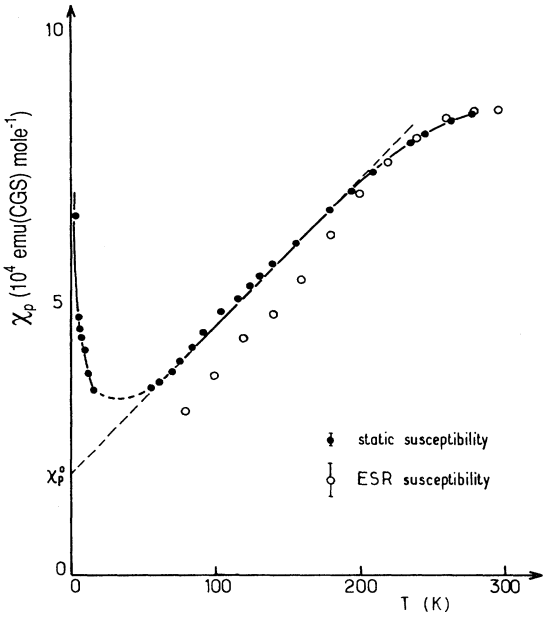

FIG. 7. Temperature dependence of the spin susceptibility of BTDMTTF-TCNQ measured by Faraday (in absolute units) and ESR methods. The RT ESR susceptibility has been adjusted to the RT Faraday susceptibility value corrected from the core diamagnetism.

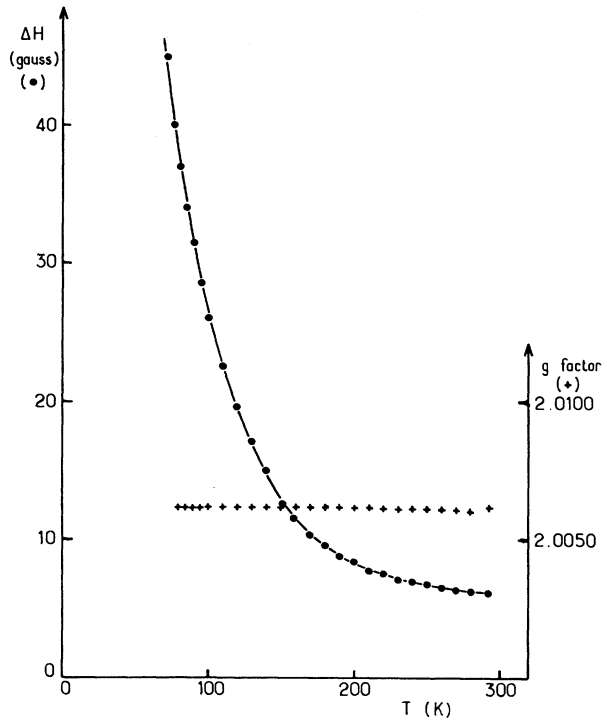

FIG. 8. Temperature dependence of the peak-to-peak ESR linewidth (ΔH) and the g factor of BTDMTTF-TCNQ for H parallel to a^*.

crease is seen in TTF-TCNQ.[2,20] The low-temperature increase of χ_p observed in Fig. 7 can be attributed to a Curie tail due to magnetic defects or impurities. No data are shown around 40 K because of the presence of a small contamination from the magnetism of solid O_2 absorbed by the sample.

Electron-spin resonance (ESR) measurements were carried out on a Varian X-band spectrometer equipped with an Oxford variable-temperature cryostat. The low-temperature experiments were carried out on a single crystal with the magnetic field (H) applied perpendicular to the (100) plane.

The detected ESR signal is Lorentzian. At RT the g tensor principal values were found to be $g_{min}=2.0028$ (for $H\|c$), $g_{int}=2.0058$ (for $H\|b$), and $g_{max}=2.0061$ (for $H\|a^*$). The RT linewidth (ΔH) along the c, b, and a^* directions is 4, 5.5, and 6 G, respectively. These linewidths are a factor of 2 smaller than the ΔH of HMTTF-TCNQ and slightly smaller than those of TTF-TCNQ.[20] This means that BTDMTTF-TCNQ is a strongly 1D electronic system.

The thermal dependence of g_{max} and ΔH_{max} is shown in Fig. 8. g_{max} does not change with temperature, while ΔH_{max} increases dramatically on cooling, making the ESR signal too broad to be detected below 80 K. This rate of increase is much larger than that observed in TTF-TCNQ, where ΔH increases by a factor of 2 between RT and 60 K.[2,20] The thermal dependence of the spin susceptibility, obtained from integration of the ESR spectrum, is also shown in Fig. 7. Within experimental errors the ESR susceptibility behaves like χ_p. This proves that the large decrease of χ_p upon cooling comes from the spin susceptibility.

VI. OPTICAL PROPERTIES: ELECTRONIC AND VIBRATIONAL SPECTRA

Measurements of finely ground KBr pellet samples with a weight concentration about 1% have been carried out using a Nicolet MX1 interferometer (350–4800 cm^{-1}) equipped with a He cryostat and a visible-UV Perkin-Elmer 350 interferometer (3850–25 000 cm^{-1}).

The absorption spectra recorded in the infrared (IR) range at 10 and 300 K are shown in Fig. 9(a). Figure 9(b) gives the mean electronic absorption coefficient at RT on a larger energy range. These spectra are similar to those of other conducting charge-transfer complexes. They are composed of a broad and intense charge-transfer band centered around 300 cm^{-1} which corresponds to the classical A-type band characteristic of mixed valence systems.[21] It must be noted that the other B-type charge-transfer band around 11 000–12 000 cm^{-1} due to the presence of doubly charged molecular sites is rather weak.

The rich vibrational spectra observed in Fig. 9(a) is characterized by the presence of vibronic lines. Most of them are a_g modes which become IR active through linear electron-molecular (e-mv) interactions.[22] Due to

the presence of both donor and acceptor mixed valence stacks two series of vibronic modes can be detected.

(i) For BTDMTTF, for which attributions are not completely established, intense vibronic modes are observed at 460, 1120, and 1335 cm^{-1}.

(ii) For TCNQ, these modes are observed at 594 ($\nu_8 a_g$), 691 ($\nu_7 a_g$), 1120 ($\nu_5 a_g$), 1335 ($\nu_4 a_g$), 1561 ($\nu_3 a_g$), and 2204 cm^{-1} ($\nu_{C\equiv N}$).[23]

Concerning the acceptor molecule, the RT frequency of the $\nu_{C\equiv N}$ vibronic line at 2204 cm^{-1} allows us to estimate a degree of charge transfer (ρ) around 0.50.[24] No qualitative change of the IR spectra is observed upon cooling down to 10 K.

The Raman spectrum at RT shows the expected totally symmetric modes corresponding to the BTDMTTF and TCNQ molecules. This spectrum is very similar to that of TTF-TCNQ.[25] From the frequency of the $a_g \nu_4 C\equiv N$ mode of the TCNQ molecule (1424 cm^{-1}), a degree of charge transfer of 0.51 ± 0.05 can be estimated.[26]

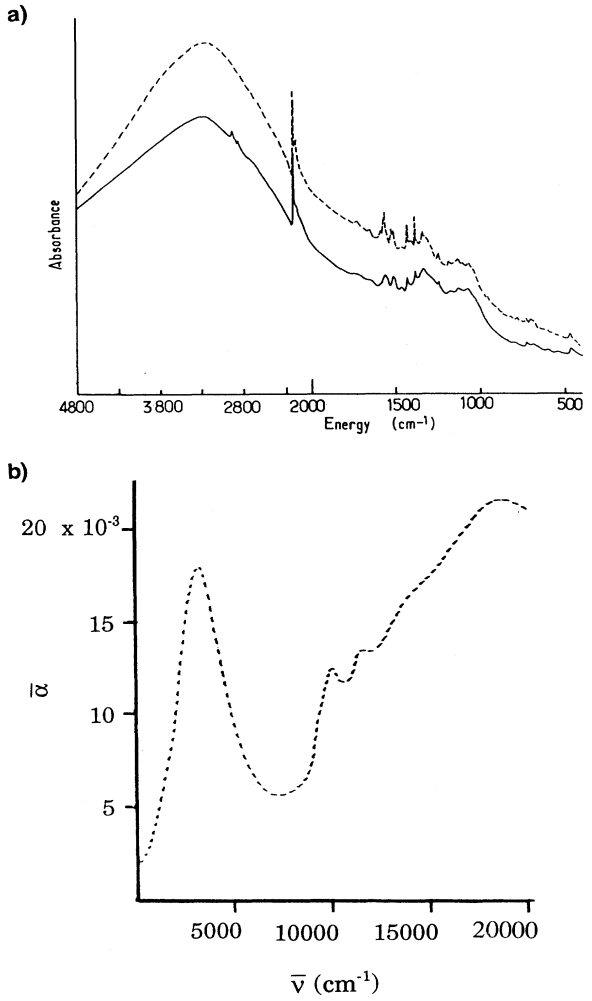

FIG. 9. (a) Infrared-absorption spectra at 10 (— — —) and 300 K (——). (b) Mean electronic absorption coefficient (α) vs a photon energy of BTDMTTF-TCNQ.

VII. X-RAY DIFFUSE SCATTERING INVESTIGATION

As in previous studies of structural instabilities in organic conductors, the x-ray diffuse scattering experiment was performed with the so-called fixed film-fixed crystal method using a monochromatized Cu $K\alpha(\lambda = 1.524$ Å) x-ray beam as incident radiation after (002) reflection on a doubly bent graphite monochromator.[27] Temperatures were regulated in the range 20 K to RT. Two needles 3 mm long in the stack direction (c), and a few tenths of a mm in the other directions, were investigated. Each sample was glued with a silver paint to a sample holder in good thermal contact with the cold finger of a He closed-circuit cryocooler. The samples were oriented with respect to the x-ray beam in such a way that the (b^*,c^*) reciprocal plane, according to the cell setting of Table I, was projected on the photographic plate. The x-ray diffuse scattering intensity was analyzed from microdensitometer readings of the photographic films.

X-ray patterns taken at RT reveal a weak diffuse scattering consisting of single diffuse lines located midway between successive layers of the main Bragg reflections perpendicular to the c direction. This diffuse scattering is more clearly revealed [see Fig. 10(a)] by the microdensitometer readings performed along c^*. At RT this scattering occurs at the reduced wave vector

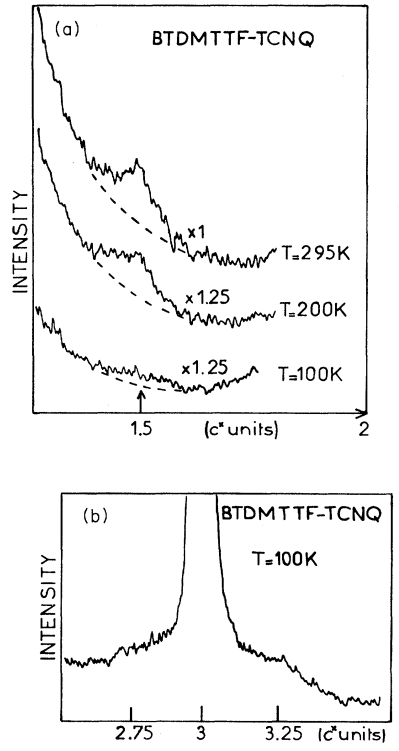

FIG. 10. (a) Microdensitometer reading along c^* of x-ray patterns from BTDMTTF-TCNQ at 295, 200, and 100 K showing the vanishing of the q_1 diffuse scattering upon cooling. (b) Microdensitometer reading along c^* of an x-ray pattern from BTDMTTF-TCNQ at 100 K showing the broad q_2 diffuse scattering.

$q_1 = 0.50 \pm 0.02 c^*$. By analogy with previous findings for charge-transfer organic salts of the TTF-TCNQ family,[4] these diffuse lines correspond to charge-density-wave (CDW) fluctuations uncorrelated from chain to chain. However, it is observed that the intensity of the q_1 diffuse scattering diminishes on cooling down and becomes undetectable below about 100 K, as shown by the microdensitometer readings of Fig. 10(a). The vanishing of the q_1 peak intensity as a function of temperature is more quantitatively illustrated in Fig. 11. In addition, a slight shift of the q_1 reduced wave vector seems to occur on cooling: at 150 K the diffuse lines no longer pass through the weak Bragg reflections due to the diffraction by the $\lambda/2$ contamination of the incident radiation. At this temperature q_1 can be estimated at $0.45 \pm 0.02 c^*$ or, within a reciprocal wave vector c^*, at $0.55 \pm 0.02 c^*$. Over all the temperature range where they are observed, the q_1 diffuse lines remain broad. At RT their half width at half maximum (HWHM) along c, $\Delta Q = 0.08$ Å^{-1} leads, to an intrachain CDW correlation length $\xi_c = \Delta Q^{-1}$ of about 12 Å (i.e., $3 \times c$).

In addition, x-ray patterns around 100 K reveal another very broad diffuse scattering at about $q_2 \approx 0.25 c^*$, as shown on the microdensitometer reading of Fig. 10(b). At the HWHM of $\Delta Q \sim 0.17$ Å^{-1} of the q_2 scattering corresponds a very short intrachain CDW correlation length $\xi_c \sim 6$ Å (i.e., $1.5 \times c$). Upon cooling from 100 K the q_2 scattering progressively vanishes while remaining broad. Upon heating from 100 K it merges into the thermal diffuse scattering originating from the Bragg reflections.

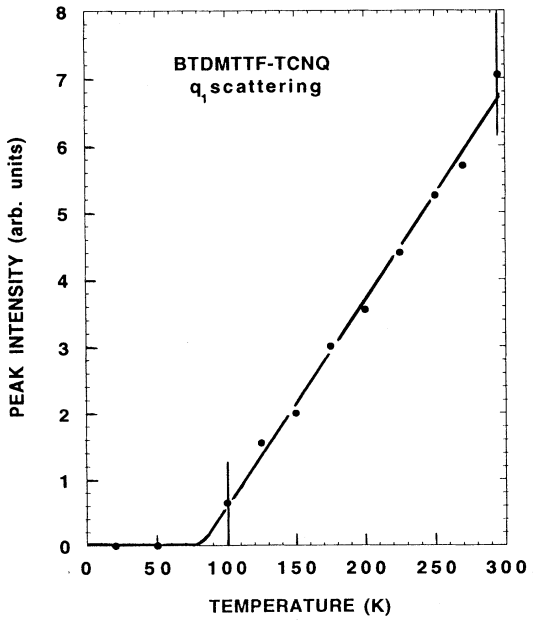

FIG. 11. Temperature dependence of the peak intensity of the q_1 diffuse scattering of BTDMTTF-TCNQ.

VIII. ELECTRONIC STRUCTURE

The electronic structure of BTDMTTF-TCNQ has been studied by means of tight-binding extended Hückel calculations.[28] A modified Wolfsberg-Helmholz formula[29] was used to calculate the nondiagonal $H_{\mu\nu}$ values. Single-ζ Slater-type orbitals were used for all atoms.[30] The exponents and $H_{\mu\mu}$ (eV) values used were 1.625 and -21.4 for C $2s$, 1.625 and -11.4 for C $2p$, 1.817 and -20.0 for S $2s$, 1.817 and -13.3 for S $2p$, 1.95 and -26.0 for N $2s$, 1.95 and -13.4 for N $2p$, and 1.30 and -13.6 for H $1s$.

The highest occupied molecular orbital (HOMO) of BTDMTTF is shown in Fig. 12. It is interesting to remark that the external sulfur (S5) orbitals do not contribute to this HOMO, which is thus very similar to that of TTF. Thus this extra sulfur atom will certainly affect the cohesion energy and vibrational properties of the system, but will not influence in a direct way the transport properties of this or other salts of BTDMTTF. In other words, even if the number of short sulfur-sulfur contacts can be larger than in isostructural HMTTF salts, for instance, these contacts will not contribute to increase the energy dispersion of the HOMO band, i.e., the partially filled band in the metallic salts. The dispersion of this band will be changed only in an indirect way because the presence of this external sulfur atom will slightly change the stacking and thus the overlap integrals between nearest-neighbor molecules. The presence of this external sulfur atom will certainly also change the donating ability of the molecule. Thus the introduction of these additional sulfur atoms is a way to modify the electron filling of the bands and the stiffness of the lattice while making only small changes in the band structure of the system. Tight-binding band-structure calculations were carried out for the RT and 130 K structures of BTDMTTF-TCNQ. The transfer integrals perpendicular to the chain direction are extremely small, so that the 3D band structure of this salt is just the superposition of those of the individual chains. The maximum dispersion along the transverse directions occurs for the TCNQ LUMO (lowest unoccupied molecular orbital) band which is smaller than 0.01 eV. As is the case for all other salts of this family, the band structure is of the inverted type and the energy dispersions at RT (130 K) are of 0.31 (0.34) and 0.56 (0.62) eV for the BTDMTTF and TCNQ bands, respectively.

With the same type of calculations the band dispersions for the donor and acceptor chains of TTF-TCNQ are 0.32 and 0.66 eV, and those of HMTTF-TCNQ are 0.34 and 0.60 eV, respectively. These calculated band-

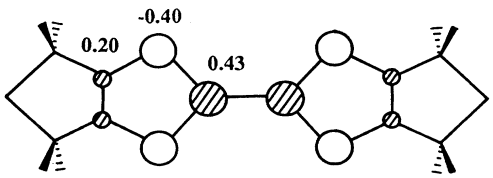

FIG. 12. HOMO of the BTDMTTF molecule.

widths are about 25% lower than the bandwidths deduced from plasma frequency measurements (i.e., 0.41 and 0.81 eV for the donor and acceptor bands of TTF-TCNQ, and 0.80 and 0.76 eV for the donor and acceptor bands of HMTTF-TCNQ according to Jacobsen[31]). These calculations show that, like other charge-transfer salts of the TTF-TCNQ family, BTDMTTF-TCNQ is a strongly 1D metal exhibiting relatively narrow donor and acceptor bands.

IX. GENERAL DISCUSSION

Let us first consider the determination of the charge transfer. Both IR and Raman frequency measurements give a charge transfer $\rho \sim 0.50$ from BTDMTTF to TCNQ. Such a value agrees with the x-ray diffuse scattering determination. This experiment shows that two CDW instabilities develop in the metallic phase of the quasi-1D conductor BTDMTTF-TCNQ. The main instability occurs at a q_1 reduced wave vector close to $0.5c^*$ and an incipient one at a q_2 reduced wave vector close to $0.25c^*$. Within experimental errors one has $q_1 = 2q_2$, and by analogy with previous studies of charge-transfer salts[4] the q_1 and q_2 wave vectors must correspond to the $4k_F$ and $2k_F$ critical wave vectors of the CDW response functions of the 1D electron gas. Such an assignment implies that there is a charge transfer of $\rho = 4k_F/c^* = 0.5 \pm 0.02$ electrons from BTDMTTF to TCNQ at RT. Although three independent determinations agree on the value of the charge transfer, let us mention that quite different values of ρ can be deduced from the bond lengths of the TCNQ molecule obtained from our RT structural refinement (i.e., $\rho = 0.65$ and 0.81 according to the equations proposed by Kistenmacher *et al.*[32] and Umland *et al.*,[33] respectively). Such a discrepancy casts some doubt on the accuracy of these bond-length–charge-transfer correlations.

The thermal variation of q_1 suggests a change of the charge transfer upon cooling. Such changes were previously observed in TTF-TCNQ and TMTTF-bromanil.[4] However, as q_1 deviates from $0.5c^*$ at RT to $0.45c^*$ or to $0.55c^*$ around 150 K, one cannot determine if the charge transfer decreases or increases upon cooling. Let us mention here that, as for TTF-TCNQ,[4] 1D tight-binding calculations predict an increase of charge transfer upon cooling. In this description the charge transfer, assuming an inverted band structure, is given by[4]

$$\rho = \frac{1}{\pi} \arccos \left[\frac{E^A - E^D}{2(|t^D| + |t^A|)} \right] , \tag{1}$$

where $t^A (t^D)$ and $E^A (E^D)$ are the intrastack transfer integral and midband energy of the acceptor (donor) band, respectively. Assuming that only t^A and t^D vary with temperature, one obtains the relative variation

$$\frac{\Delta\rho}{\rho} = \frac{2}{\pi\rho} \left[\frac{|\Delta t^A| + |\Delta t^D|}{|t^A| + |t^D|} \right] \cot \frac{\pi\rho}{2} . \tag{2}$$

Our tight-binding band-structure calculation shows that the acceptor bandwidth ($4t^A$) increases from 0.56 to 0.62 eV, and that the donor bandwidth ($4t^D$) increases from 0.31 to 0.34 eV between 295 and 130 K. This leads to a relative variation of charge transfer of $\Delta\rho/\rho = 12.5\%$, which agrees quite well with that given by the relative shift of the q_1 wave vector measured between 295 and 150 K, namely $\Delta q_1/q_1 \sim 10\%$.

It is interesting to remark that although the BTDMTTF molecule resembles the HMTSF and HMTTF molecules, and that the crystal structure of their TCNQ salts exhibits the same chess board array between the donor (D) and acceptor (A) stacks, the charge transfers are quite different: $\rho = 0.5$ in BTDMTTF-TCNQ, $\rho = 0.72$ in HMTTF-TCNQ, and $\rho = 0.74$ in HMTSFT-TCNQ. In charge-transfer salts, the relative stability of the DA array has been interpreted[34] as the result of the competition between the Madelung energy of charged chains and the van der Waals energy of metallic chains composed of highly polarizable molecules: the former interaction favoring the alternation of D and A stacks in the two lateral directions, and the latter interaction favoring the formation of sheets of D or A stacks. However, the observation of a chess board array in a salt containing the highly polarizable BTDMTTF molecule and having a reduced charge transfer $\rho \sim 0.5$, while other salts like TTF-TCNQ having about the same charge transfer and less polarizable molecules adopt a layered array, suggests that additional features should be considered. It could well be that, because of its sizable rate of decrease with the interchain distance (i.e., as R^{-6}), the van der Waals interaction in fact diminishes in salts containing large molecules despite the increase of their polarizability. If the Madelung energy term dominates, the chess board structure of the HMTT(S)F and BTDMTTF-TCNQ salts can then be understood.

The low value of the RT conductivity (Sec. IV) and the high value of the RT spin susceptibility (Sec. V) show that BTDMTTF-TCNQ is a 1D highly correlated metal, comparable to TTF-TCNQ. Such a result could be surprising because although the D and A bandwidths are comparable to those of TTF-TCNQ according to our calculations (se Sec. VIII), one expects the Coulomb interactions to be less important on the BTDMTTF stacks than on the TTF ones. The reason is that because of its two sulfur-containing external rings, the BTDMTTF molecule should be more polarizable than the TTF one.[35] However, the slight decrease of charge transfer from TTF-TCNQ ($\rho = 0.55$) to BTDMTTF-TCNQ ($\rho = 0.5$) could compensate the decrease of such Coulomb interactions, because for $\rho = 0.5$ only comparable values of U (intramolecular Coulomb interactions) and V_1 (first-neighbor Coulomb repulsions) are required to achieve a Wigner localization of charges, while Coulomb interactions of longer range (i.e., V_j going beyond the first neighbor) are required to achieve such a charge localization for $\rho > 0.5$.[36]

Because of the existence of a RT $4k_F$ instability, BTDMTTF-TCNQ resembles the other charge-transfer salts of this family with $\rho = 0.5$ such as TMTTF-DMTCNQ and TMTSF-DMTCNQ.[4] In the high-temperature (T) limit, the intensity of the $4k_F$ x-ray scattering $I(4k_F)$, is related to the $4k_F$ CDW response

function $\chi_\rho(4k_F)$ through the classical relationship[4]

$$I(4k_F)=k_B T\chi_\rho(4k_F) . \quad (3)$$

The vanishing of $I(4k_F)$ at about 80 K (Fig. 11) thus reflects the drop of $\chi_\rho(4k_F)$ at low temperature. This effect could be attributed to the variation of the charge transfer with temperature: as ρ deviates from 0.5, the $4k_F$ CDW instability becomes less and less stable because sizable Coulomb interactions V_j going beyond the first neighbors ($j>1$) are now required to localize the charges. In this respect it is interesting to note that the vanishing of $I(4k_F)$ when T decreases is much more dramatic for BTDMTTF-TCNQ (where ρ varies with temperature) than for TMTSF-DMTCNQ (where ρ remains 0.5).[37]

However, with respect to the other charge-transfer salts of the TTF-TCNQ family,[4] BTDMTTF-TCNQ is unique because it does not exhibit a well-defined $2k_F$ CDW instability which becomes critical at low temperature. Such a finding is in agreement with the transport measurements, which do not reveal the existence of a Peierls transition. This means either that the $2k_F$ CDW response remains always very weak or that the electron-phonon coupling is so small that the $2k_F$ electron-hole instability expected for a 1D electron gas cannot be transmitted to the lattice degrees of freedom which are probed in the x-ray diffuse scattering experiment. As the electronic properties of BTDMTTF-TCNQ strongly resemble those of TTF-TCNQ, there is no apparent reason for which there will be no $2k_F$ electron-hole instability. Indeed, the observation of a very weak q_2 scattering around 100 K shows that this instability really occurs. We suggest that, because of the close packing of the BTDMTTF and TCNQ molecules, the transverse-acoustic-like modes of deformation of the stacks, generally involved in the $2k_F$ Peierls distortion of the organic charge transfer salts,[4] are too stiff to provide a large enough reduced electron-phonon-coupling constant (λ defined in Ref. 38) able to sustain the $2k_F$ Peierls instability. In other words, the elastic energy cost associated with the Peierls transition will overcome the $2k_F$ electronic energy gain in BTDMTTF-TCNQ. As noted in Secs. III and VIII, although with apparently no effect on the electronic band structure, there are several S $\cdots$ N, S $\cdots$ C, and C-H $\cdots$ N, intermolecular contacts shorter than the sum of the van der Waals radii along the interstack directions. A closer look at the crystal structure shows that the (CN)-C-(CN) angle of the TCNQ molecule of BTDMTTF-TCNQ (118.2°) is larger than in other salts of this series which exhibit a $2k_F$ Peierls transition: 117.3° in HMTTF-TCNQ, 116.0° in TMTTF-TCNQ, 115.0° in HMTSF-TCNQ, and 114.5° in TMTSF-TCNQ. This clearly shows that the donor and acceptor chains in BTDMTTF-TCNQ are more strongly interlocked [see Fig. 2(a)], and thus that the distortion should cost more elastic energy than for the other charge-transfer salts.

Such interstack contact terms could be the key parameter which controls the occurrence of a Peierls transition in charge-transfer salts, in spite of the $2k_F$ divergence of the electron-hole response function of the 1D electron gas. The stiffening of such contact terms under pressure could be the clue to understanding the rapid disappearance of the $2k_F$ Peierls transition of TMTSF-DMTCNQ above 10 kbar.[5] Even for salts which undergo a $2k_F$ CDW Peierls distortion, such interactions could explain the relatively small value ($\lambda\sim 0.2$) found for the reduced electron-phonon-coupling constant of the acoustic mode of deformation of the TSF stack in TSF-TCNQ.[39] Similar small values of λ were suggested from an analysis of the physical properties of TTF-TCNQ.[40]

It is also interesting to compare BTDMTTF-TCNQ with HMTSF-TCNQ (Ref. 17) and TTeF-TCNQ,[9] which both keep a high conductivity down to low temperatures. While HMTSF-TCNQ undergoes a weak $2k_F$ Peierls transition at about 24 K, and TTeF-TCNQ develops critical $2k_F$ structural fluctuations which do not condense into a Peierls ground state,[4] BTDMTTF-TCNQ does not exhibit critical $2k_F$ structural fluctuations. In this respect it would be interesting to further stabilize the metallic state of BTDMTTF-TCNQ by applying hydrostatic pressure.

Although BTDMTTF-TCNQ does not undergo a Peierls transition, the thermal variation of its electronic properties presents anomalies around 175 and 25 K. Around 175 K the rate of increase of the electrical conductivity and of the thermopower saturate and the ESR linewidth begins to increase sizably. An upturn in the thermal variations of the electrical conductivity and thermopower is observed around 25 K. The physical origin of these electronic anomalies is not understood. The 175 K anomaly should be correlated with structural modifications of the unit cell. Figure 3 shows that below 175 K the stack periodicity c decreases more rapidly, and that a significant modification of the stack packing occurs (a and b decrease more rapidly while β increases more rapidly), leading to a larger rate of decrease of the unit-cell volume. Curiously, the c parameter contraction, instead of increasing the intrachain electrical conductivity (as generally occurs in pressurized charge-transfer salts[2]), nearly stops its thermal variation. However, the large increase of the ESR linewidth could be explained by an increase of interchain electronic interactions due to the structural modification. Transverse conductivity measurements should be performed in order to clarify more precisely the effect of the interchain coupling. The slight increase of the resistivity and the rapid vanishing of the thermopower below 25 K could be the onset of weak-localization effects due to some residual disorder.

X. CONCLUDING REMARKS

We have prepared a charge-transfer salt BTDMTTF-TCNQ which remains metallic down to low temperatures. IR, Raman, and x-ray diffuse scattering measurements show that the charge transfer is of $\rho\sim 0.5$ electrons from the BTDMTTF donor to the TCNQ acceptor. Band-structure calculations show that this salt is a narrow-band 1D conductor similar to TTF-TCNQ. The low value of the conductivity, and the high value of the

spin susceptibility as well as the observation of a $4k_F$ CDW instability around RT, prove that this metal is highly correlated. However, in contrast with other salts of the TTF-TCNQ family, BTDMTTF-TCNQ does not exhibit critical $2k_F$ structural fluctuations. We interpret the absence of a $2k_F$ CDW Peierls transition as being due to the strong interlock of the BTDMTTF and TCNQ molecules which renders the elastic cost of the structural distortion too prohibitive. We attribute this special situation to the external sulfur atom of the BTDMTTF molecule. Although this atom does not influence the band structure of the BTDMTTF-TCNQ salt because its site does not contribute to the HOMO of the donor, its interactions with the other atoms influence the crystal packing and the cohesion energy of the crystal.

ACKNOWLEDGMENTS

We would like to thank Dr. L. Artus (Institut Jaume Almera, CSIC) for carrying out the Raman spectrum. This work was supported by a grant from Programa Nacional de Quimica Fina, (CIRIT-CICyT) Spain (QFN93-4510-CO1) and the Human Capital and Mobility Program of the UE (ERBCHRX CT93-0271). Work at J. Hopkins University was supported by a grant from the National Science Foundation (DMR-9223481).

[1]J. Ferraris, D. O. Cowan, V. V. Walatka, and J. H. Perlstein, J. Am. Chem. Soc. **95**, 948 (1973); L.B. Coleman, M. J. Cohen, D. J. Sandman, F. G. Yamagishi, A. F. Garito, and A. J. Heeger, Solid State Commun. **12**, 1125 (1973).

[2]D. Jérome and H. J. Schulz, Adv. Phys. **31**, 299 (1982).

[3]*Highly Conducting Quasi-One-Dimensional Organic Crystals,* edited by E. Conwell, Semiconductors and Semimetals Vol. 27 (Academic, New York, 1988).

[4]J. P. Pouget, in *Highly Conducting Quasi-One-Dimensional Organic Crystals* (Ref. 3), p. 87.

[5]A. Andrieux, P. M. Chaikin, C. Duroure, D. Jerome, C. Weyl, K. Bechgaard, and J. P. Andersen, J. Phys. (Paris) **40**, 1199 (1979).

[6]D. Jerome, A. Mazaud, M. Ribault, and K. Bechgaard, J. Phys. Lett. (France) **41**, L-95 (1980).

[7]T. Ishiguro and K. Yamagi, *Organic Superconductors,* Springer Series in Solid State Sciences Vol. 88 (Springer-Verlag, Berlin, 1990).

[8]L. Brossard, M. Ribault, L. Valade, and P. Cassoux, Physica **143B**, 378 (1986); J. Phys. (Paris) **50**, 1521 (1989).

[9]D. O. Cowan, M. D. Mays, T. J. Kistenmacher, T. O. Poehler, M. O. Beno, A. M. Kini, J. M. Williams, Y. K. Kwok, K. D. Carlson, L. Xiao, J. J. Novoa, and M. H. Whangho, Mol. Cryst. Liq. Cryst. **181**, 43 (1990).

[10]A. Ugawa, K. Iwasaki, A. Kawamoto, K. Yakushi, Y. Yamashita, and T. Suzuki, Phys. Rev. B **43**, 14 718 (1991).

[11]N. Santaló, J. Veciana, and C. Rovira, Tetrahedron Lett. **1989**, 7249; C. Rovira, J. Veciana, N. Santaló, Tarrés, J. Cirujeda, E. Molins, J. Llorca, and E. Espinosa, J. Org. Chem. **59**, 3307 (1994).

[12]N. Santaló, J. Tarrés, E. Espinosa, J. Llorca, E. Molins, J. Veciana, C. Rovira, M. Mays, S. Yang, D. O. Cowan, C. Garrigou-Lagrange, J. Amiell, P. Delhaes, and E. Canadell, Synth. Met. **55-57**, 2050 (1993).

[13]P. Main, G. Germain, and G. Woolfson (unpublished).

[14]G. M. Sheldrick, Computer code SHELX76, Program for Crystal Structure Determination, University of Cambridge, England, 1976.

[15]R. H. Blessing, J. Appl. Cryst., **22**, 396 (1989).

[16]G. M. Sheldrick, Computer code SHELX93, University of Cambridge, England, 1993.

[17]A. N. Bloch, D. O. Cowan, K. Bechgaard, R. E. Pyle, R. H. Banks, and T. O. Poehler, Phys. Rev. Lett. **34**, 1561 (1975); T. E. Philips, T. J. Kistenmacher, A. N. Bloch, and D. O. Cowan, J. Chem. Soc. Chem. Commun. **1976**, 334.

[18]R. L. Greene, J. J. Mayerle, R. Schumaker, G. Castro, P.M. Chaikin, S. Etemand, and S. La Placa, J. Solid State Commun. **20**, 943 (1976); D. Chasseaux, G. Comberton, J. Gaultier, and C. Hauw, Acta Crystallogr. Sec. B **34**, 689 (1978).

[19]F. H. Herbstein, in *Perspectives in Structural Chemistry,* edited by J. D. Dunitz and J. A. Ibers (Wiley, New York, 1971), p. 166.

[20]J. C. Scott, in *Highly Conducting Quasi-One-Dimensional Organic Crystals* (Ref. 3), p. 385.

[21]J. B. Torrance, in *Chemistry and Physics of One Dimensional Metals,* Vol. 25 of *NATO Advanced Study Institute Series B: Physics,* edited by H. J. Keller (Plenum, New York, 1977), p. 137.

[22]M. J. Rice, V. M. Yarstev, and C. S. Jacobsen, Phys. Rev. B **34**, 3683 (1986).

[23]C. Garrigou-Lagrange, M. Lequan, A. M. Lequan, and V. M. Yartsev, J. Chim. Phys. **90**, 1749 (1993).

[24]J. S. Chappell, A. N. Bloch, W. A. Bryden, M. Maxfield, T. O. Poehler, and D. O. Cowan, J. Am. Chem. Soc. **103**, 2442 (1981).

[25]H. Kuzmany and B. Kundu, *Quasi One Dimensional Conductors,* edited by S. Basiric, A. Bjelis, J. R. Cooper, and B Leontic, Lecture Notes in Physics Vol. 95 (Springer, Berlin, 1979), p. 259.

[26]H. Kuzmany and M. Elbert, Solid State Commun. **35**, 597 (1981).

[27]S. K. Khanna, J. P. Pouget, R. Comes, A. F. Garito, and A. J. Heeger, Phys. Rev. B **16**, 1468 (1977).

[28]M.-H. Whangbo and R. J. Hoffmann, J. Am. Chem. Soc. **100**, 6093 (1978).

[29]J. H. Ammeter, H.-B. Bürgi, J. Thibeault, and R. Hoffmann, J. Am. Chem. Soc. **100**, 3686 (1978).

[30]E. Clementi and C. Roetti, At. Data Nucl. Data Tables **14**, 177 (1974).

[31]C. S. Jacobsen, Mat. Fys. Medd. Dan. Vid. Selsk. **41**, 251 (1985).

[32]T. Kistenmacher, T. J. Emge, A. N. Bloch, and D. O. Cowan, Acta Crystallogr. Sec. B **38**, 1193 (1982).

[33]T. C. Umland, S. Allie, T. Kuhlmann, and P. Coppens, J. Phys. Chem. **92**, 6456 (1988).

[34]D. Debray, R. Millet, D. Jerome, S. Barisic, J. M. Fabre and L. Giral, J. Phys. Lett. (France) **38**, L227 (1977).

[35]Such an assertion is supported by electrochemical measure-

ments for TTF and BTDMTTF (in DMF with 0.1 *M* tetrabuthylammonium hexafluorophosphate). The oxidation potentials (measured with Pt electrodes at a rate of 200 mV s^{-1} vs saturated calomel electrode) for TTF [$(E_{1/2})_1=0.39$ V $(E_{1/2})_2=0.62$ V] and BTDMTTF [$(E_{1/2})_1=0.55$ V, $(E_{1/2})_2=0.72$ V] prove that the difference of potential $\Delta E_{1/2}$ decreses from TTF (0.23 V) to BTDMTTF (0.17 V). Such a decrease can be related to an increase of the intramolecular polarizability from TTF to BTDMTTF, and to a decrease of the intramolecular Coulomb interaction term *U*.

[36]J. Hubbard, Phys. Rev. B **17**, 494 (1978).

[37]J. P. Pouget, Chem. Scr. **17**, 85 (1981).

[38]In the standard theory of the Peierls transition (Ref. 2), the reduced electron-phonon-coupling constant λ amounts to $g^2N(E_F)/\hbar\omega(2k_F)$, where g is the electron-phonon-coupling constant, $N(E_F)$ is the density of states at the Fermi level, and $\omega(2k_F)$ is the bare frequency of the phonon mode which presents the $2k_F$ instability. Here the discussion concerns the stiffening of $\omega(2k_F)$ for the transverselike acoustic mode of the deformation of the stacks due to their interlock.

[39]J. P. Pouget, S. Ravy, and B. Hennion, Phase Trans. **30**, 5 (1991).

[40]S. Barisic and A. Bjelis, in *Theoretical Aspects of Band Structures and Electronic Properties of Pseudo-One-Dimensional Solids,* edited by H. Kanimura (Reidel, Dordrecht, 1985), p. 49.

[41]J. P. Pouget, D. O. Cowan, and M. D. Mays (unpublished).